




Article

A Non-Invasive In Situ Spectroscopic Analysis of Cinnabar Minerals to Assist Provenance Studies of Archaeological Pigments

Silvia Pérez-Diez ¹, Cheyenne Bernier ², Javier G. Iñáñez ³ and Maite Maguregui ^{4,*}

¹ Department of Analytical Chemistry, Faculty of Science and Technology, University of the Basque Country UPV/EHU, 48080 Bilbao, Spain

² Department of Humanities, University of Bordeaux Montaigne, 33607 Bordeaux, France

³ Department of Geography, Prehistory and Archaeology, University of the Basque Country UPV/EHU, 01006 Vitoria-Gasteiz, Spain

⁴ Department of Analytical Chemistry, Faculty of Pharmacy, University of the Basque Country UPV/EHU, 01006 Vitoria-Gasteiz, Spain

* Correspondence: maite.maguregui@ehu.eus

Abstract: This study presents a non-invasive in situ methodology based on the use of portable elemental (energy dispersive X-ray fluorescence spectroscopy, EDXRF) and molecular (Raman spectroscopy) spectroscopic-based instrumentation as a tool to obtain preliminary information to assist subsequent provenance studies of archaeological cinnabar pigments in the laboratory. In this work, six cinnabar mineral ores, extracted from the Almadén mining district and an original raw pigment coming from the Archaeological Park of Pompeii have been analyzed. As the detection capacities and spectral resolution of the portable instruments are usually poorer than the equivalent benchtop equipment, a comparative study of the in-situ and laboratory results was conducted. Afterward, chemometric data treatment was performed considering both the molecular and elemental information. According to the elemental results, it was not possible to find a strong concordance between the cinnabar ores and the pigment from Pompeii, suggesting the need for additional methodologies in the laboratory (isotope ratio analysis) to complete a proper provenance study. However, this approach was useful to classify the ores according to their mineralogical differences. Therefore, this methodology could be proposed as a useful tool to conduct a representative sampling of the cinnabar mineral ores to be considered in a provenance study of archaeological cinnabar pigments.

Keywords: cinnabar; Pompeii; mineral ores; handheld X-ray fluorescence spectroscopy; portable Raman spectroscopy; in-situ analysis; provenance studies



Citation: Pérez-Diez, S.; Bernier, C.; Iñáñez, J.G.; Maguregui, M. A Non-Invasive In Situ Spectroscopic Analysis of Cinnabar Minerals to Assist Provenance Studies of Archaeological Pigments. *Crystals* **2023**, *13*, 207. <https://doi.org/10.3390/cryst13020207>

Academic Editor: Sergey V. Krivovichev

Received: 30 December 2022

Accepted: 18 January 2023

Published: 23 January 2023



Copyright: © 2023 by the authors. Licensee MDPI, Basel, Switzerland. This article is an open access article distributed under the terms and conditions of the Creative Commons Attribution (CC BY) license (<https://creativecommons.org/licenses/by/4.0/>).

1. Introduction

The earliest material testimonies of the use of cinnabar in burials and symbolic contexts, mural paintings and ceramics date back to the Neolithic. For instance, a Neolithic burial (3000 BC) of Palencia (Spain) is claimed to be among the first evidence of the deliberate use of cinnabar in human records, while Argaric Culture tombs (southeast Spain, 2200–1500 BC) are also known for the presence of cinnabar [1]. In addition, the earliest examples of the use of cinnabar as a pigment in wall paintings and ceramics are those of the Neolithic site of Çatalhöyük (8000–7000 BC, Turkey) [2,3].

Although cinnabar could have already been known as a pigment by Greeks since the 6th century BC and even before in Asia Minor, it was not employed in Mesopotamia nor Egypt [4] until the Late Period (664–332 BC) [5]. In Roman times, a lavish application of cinnabar on the wall paintings of a domus was vivid proof of the wealthy status of the families who could afford this costly red pigment [6].

Several mining sources are known to have been exploited throughout the world in different periods, but only few of them were already active since Antiquity, namely Ephesos, Iberia (probably Georgia and not Spain) [7,8], Sisapo (Almadén), Colchis, Carmania (present-day Iran), Ethiopia and Dardania (current Kosovo) [8,9]. Besides these mining ores, already described in Roman times, other deposits are located in Idria (Slovenia) [10], Monte Amiata (Italy), Moschellandsberg (Germany) and Genepy (France) [11]. Although the mines of Idria, Monte Amiata, Moschellandsberg and Genepy are considered to have been exploited as well by Romans, they lack of consistent archaeological studies. In addition, the first allusions to Idria and Monte Amiata as cinnabar ores are to be tracked in Christopher Columbus' records [11].

According to Pliny the Elder, the cinnabar mined in Ephesos was substituted in the 1st century BC by the Hispanic ore of Almadén [9], which has always been considered the main mineral source for the pigment employed in the wall paintings of Pompeii, the case study of this work, according to the documental evidence.

The Almadén mining district is located in the central part of Spain, in Ciudad Real (Castilla-La Mancha), 300 km southern from Madrid. The flourishing Roman municipium of Sisapo, as cited by Pliny [9], was first established in the Late Bronze Age and certain archaeological remains dated the mining activity in Almadén back to the 8th century BC. The mines were exploited, only when the emperor considered it pertinent, by the *socii sisaponensis*. A certain quantity was extracted (up to 100 net pounds per year). Then, the mines were locked until by the governor of the Baetica province. Afterward, the manufacture of the pigment was performed in Rome [12]. The prices reached by this fine red substance had to be limited by law to 70 sesterces per pound.

Three main geological deposit phases can be distinguished in Almadén, which took place during the Late Precambrian, the Paleozoic and the Late Cenozoic [13]. The formation of cinnabar is linked to surface volcanism in hydrothermal deposits of low pressure and temperature [10,14]. Cinnabar crystallization takes place in cracks and cavities of sandstone, limestone, or volcanic rocks. It is often associated with other minerals such as quartz (SiO_2), gypsum ($\text{CaSO}_4 \cdot 2\text{H}_2\text{O}$), calcite (CaCO_3), pyrite (isometric FeS_2), sphalerite (ZnS), barite (BaSO_4), orpiment (As_2S_3), realgar (As_4S_4), marcasite (orthorhombic FeS_2) and stibnite (Sb_2O_3), as well as aluminosilicates [10,15–17]. In Almadén, cinnabar is often found in the veins of quartzites [3,14,16].

Depending on the geological provenance of the cinnabar, the presence of trace elements varies greatly, making it a valuable asset to trace its origin. Hence, plenty of isotopic studies concerning the provenance of the cinnabar used as a pigment in different locations of the Roman territory have arisen. Higuera et al. performed the first Pb isotope ratio analysis of the cinnabar of the Almadén deposits (Almadén, El Entredicho and Las Cuevas) [18]. Later on, Mazzocchin et al. studied the Pb isotopic composition of cinnabar samples taken from the Roman villas of Verona, Vicenza, Montegrotto, Padova, Pordenone and Trieste; as well as the Insula del Centenario and the Casa del Bracciale D'Oro (Pompeii) and reference samples from Almadén, Monte Amiata and Idria. They concluded that all the samples were of Spanish origin: either from a precise region (e.g., Río Tinto cinnabar in the Villa di S. Cosimo, Verona) or a mixture of cinnabar ores coming from different Spanish mines and subsequently mixed, ground and purified in Rome [19]. However, this approach is not adequate for Pompeian mural paintings, since a recent study has demonstrated that the collapse of the ancient lead pipe system after the 79 AD eruption would have induced a leaching of the metal and subsequently transference to the buried elements, thus modifying the original Pb isotopic ratio ($^{206}\text{Pb}/^{207}\text{Pb}$) [20].

On the other hand, S isotope ratio analysis is indeed appropriate for the identification of the origin of the cinnabar used in the Vesuvian area and there have already been some advances to this extent. Tsantini et al. applied this method to identify the origin of the cinnabar used in Roman wall paintings of Baetulo (present-day Badalona, Spain), taking into account other minor cinnabar outcrops within the Spanish territory (e.g., Asturias) [3]. The authors noted that Almadén's cinnabar could have been formed due to

different geological (e.g., hydrothermal alterations in volcanic rocks) or biogenic processes, thus the isotope variability in this district might be relevant. It surely differs among the three main bodies: mean $\delta^{34}\text{S}$ of San Nicolás = $0.2 \pm 1.1\%$, San Francisco = $8.1 \pm 0.7\%$ and San Pedro = $5.9 \pm 1.0\%$. Finally, the mean $\delta^{34}\text{S}$ value of the cinnabar pigments was $12.46 \pm 2.1\%$, in agreement with the Almadén or Asturias (especially Tarna or Caravia) mines, which are the second more extended cinnabar ores in Spain.

Finally, Hg isotopic analyses have also been performed, which proved a mass-dependent fractionation during ore retorting. $\delta^{202}\text{Hg}$ of the ore sampled at Almadén varied from -0.92 to 0.15‰ , whereas the retorted ore and liquid metallic mercury were enriched in $\delta^{202}\text{Hg}$ in 1.90‰ and 0.67‰ , respectively. El Entredicho deposit ranges from $\delta^{202}\text{Hg}$ of -1.73 (highly negative) to -0.46‰ . Regarding Las Cuevas, the $\delta^{202}\text{Hg}$ varied from -0.90 to -0.10‰ [14].

Bearing in mind the high variability of the results obtained through isotopic analyses of cinnabar minerals, a first mineralogical study of different samples extracted from the same mining district becomes essential to select the most appropriate specimens that represent the aforementioned variability. Therefore, in this work, a non-invasive analytical methodology, including mineralogical (Raman spectroscopy, X-ray diffraction) and elemental analysis (EDXRF), has been applied to cinnabar ores of the Almadén mining district (Almadén, El Entredicho, Las Cuevas) and to a pigment recovered from the excavations of the Archaeological Park of Pompeii. Afterward, canonical discriminant analysis (CDA) and principal component analysis (PCA) were performed considering both Raman and EDXRF data. The results here presented offer a better understanding of the most popular source of the cinnabar mineral employed to manufacture the Roman pigment. The joint application of portable and benchtop Raman and EDXRF spectrometers allowed to verify the usefulness of the portable devices for their in-situ application to obtain representative samples for a future isotopic analysis, bearing in mind the heterogeneities of the mining district of Almadén, as summarized above.

2. Materials and Methods

2.1. Samples

The cinnabar ores studied in this work correspond to the mining district of Almadén. Three locations have been sampled: Almadén, Las Cuevas and El Entredicho (see Figure 1). Two mineral fragments were considered from each location. In addition, a raw cinnabar pigment recovered from the excavations of the Archaeological Park of Pompeii was analyzed. This pigment was probably ready to be used by a person who was painting a mural right before the Mt. Vesuvius eruption in 79 AD. It is well-known that some mural paintings of the ancient city were under restoration due to the effects of the earthquake that took place in 62 AD [21,22].



Figure 1. Map of the Almadén mining district and the location of the ore fragments. Adapted with permission from Gray et al. [14]. 2013. Elsevier.

2.2. Instruments and Analytical Approach

EDXRF spectroscopy was employed to perform an elemental analysis of the cinnabar ores and the Pompeian pigment. Two instruments were employed: a Tracer 5 g (Bruker Nano GmbH, Berlin, Germany) handheld EDXRF (HH-EDXRF) spectrometer and a M4 TORNADO EDXRF spectrometer (Bruker Nano GmbH, Berlin, Germany).

The TRACER 5g instrument presents a Rh thin window X-ray tube, whose maximum voltage is 50 kV, and a 1- μm graphene detector window. The emitted X-ray beam can be collimated to 3 or 8 mm. In this case, the 8-mm collimator was selected for the measurements. The analyzer uses a 20 mm² high-resolution silicon drift detector (SDD), which allows achieving an energy resolution of 140 eV (FWHM of the Mn K $_{\alpha}$ line). Additionally, it has an interactive touchscreen and an inbuilt VGA CMOS camera with storage capacity for up to 5 photos per essay. Two spectra were obtained for each point in order to increase the detection threshold of light elements. For heavy elements, voltage was set at 45 kV and the current was fixed at 15 μA . The spectral information was acquired during 60 s using a Ti 25 μm -Al 300 μm filter. The instrumental parameters for the detection of light elements ($Z < 25$) were lower voltage (13 kV), higher current (40 μA) and longer acquisition time (120 s). The spectra were acquired and analyzed using the following software: Bruker Remote Control, Bruker Instrument Tools, Spectra EDX Launcher and Artax 8.0.0.476.

Three randomly selected areas were measured directly (double acquisition for light and heavy elements detection) on each sample. Due to the small amount of sample, it was not possible to analyze the historical pigment by HH-EDXRF.

The M4 TORNADO EDXRF spectrometer allows measuring at 1 mm (mechanical collimation) and down to 25 μm (poly-capillary lens) of lateral resolution. In order to compare the results acquired with both EDXRF spectrometers and to be in the same scale of lateral resolution (millimetric), the benchtop measurements were conducted with the mechanical collimation. The apparatus uses two XFlash silicon drift detectors to resolve the energy of the Mn-K $_{\alpha}$ line to 145 eV. Two video microscopes were employed for the focusing process; the first examined the sample at a low magnification (1 cm² area), and the second carried out the final focusing (1 mm² area) to perform the analysis. A multi-point strategy was applied to measure the cinnabar ores and the archaeological pigment. Concretely, 6 measurements were conducted directly on each mineral sample. Moreover, apart from direct measurements, isolated cinnabar powders obtained from the mineral ore sample were also measured with the benchtop instruments. In this case, 8 measurements were acquired per each powdered sample and three additional ones in the case of the Pompeian cinnabar pigment. Each measurement with the benchtop instrument was acquired during 100 s.

Apart from single point measurements, the benchtop EDXRF spectrometer was also used for imaging studies of the mineral samples, obtaining the distribution maps (hypermaps) of the elements detected. The mapping process took place at a 20-ms scan rate with a 20- μm step size. A prior deconvolution of the signals in the total spectrum representing the entire mapped area was carried out to create the elemental images. The distribution map of each element was then displayed as a function of each K $_{\alpha}$ line's intensity.

Principal Component Analysis (PCA) was conducted using the datasets obtained from the single point measurements acquired with both EDXRF spectrometers. For that, R (3.0) and RStudio (2021.09.1) were used. Semi-quantitative data (% w/w normalized) were used to construct the datasets (direct measurements of mineral samples and powdered mineral samples respectively) acquired with the benchtop instrument. A two-step technique that first calculates the sample composition from the net peak intensities was utilized. The resulting XRF spectra were simulated (forward computed) using key parameters based on an estimated sample composition (FP). Standardless FP quantification was applied in this instance. These simulated spectra were then compared with the measured spectra and matched by iterating the sample properties. No specific corrections were incorporated to the FP method already implemented in the instrument. Hence, the results can only be considered semi-quantitative.

The dataset prepared from the spectral information acquired with the handheld instrument includes the counts of each element detected in a spectrum normalized by the total number of counts in the spectrum.

Concerning the molecular composition of the cinnabar ores and the pigment, the results obtained using two Raman spectrometers were compared: a portable innoRam™ (B&W Tek, Inc., Newark, NJ, USA) and an inVia confocal microscope (Renishaw, Gloucestershire, UK).

The portable Raman spectrometer employed uses a 785 nm wavelength excitation laser of CleanLaze® technology. Additionally, it has a CCD detector that is thermoelectrically cooled to $-20\text{ }^{\circ}\text{C}$ in order to minimize energy loss and increase dynamic range. A 4.0 cm^{-1} spectral resolution (measured at the 912 nm line) is achieved thanks to double pass optical transmission. The spectra were obtained between 65 and 3000 cm^{-1} . Spectral acquisition was made using the software BWSpec™ version 4.0215.

To determine if the spectral information acquired during the direct measurements of the mineral ores using the portable Raman spectrometer allows discriminating cinnabar minerals depending on their sampling location, canonical discriminant analysis (CDA) was performed. For that, the whole spectral range acquired was considered. JMP® 13.2.0 software was used (SAS Institute Inc., Cary, NC, USA).

The confocal Raman apparatus is equipped with a CCD detector cooled by the Peltier effect ($-70\text{ }^{\circ}\text{C}$). A Leica DMLM microscope with a choice of long-range lenses ($5\times$, $20\times$, $50\times$ and $100\times$) is paired with the spectrometer. Confocality enables the microscope to achieve its highest lateral resolution. The microscope has a motorized XYZ turntable with X and Y axis position sensors (Renishaw). Three excitation lasers are available: 785, 633, and 532 nm. To be able to compare the results with the spectra acquired with the portable instrument and to avoid any fluorescence problems, the measurements were all carried out with the near-infrared laser (785 nm) with a power source of 350 mW (output power) and around 150 mW (setting at 100% the laser power) on the sample surface.

The interpretation of the spectra was performed through free databases such as RRUFF [23] and the evaluation and processing of the spectra was conducted using the software WiRE 4.2 (Renishaw) and OMNIC version 7.2.

Ore samples were measured by Raman directly on the specimens and using the isolated powder from the cinnabar veins of the mineral ore. The resulting powders scraped from Almadén and Las Cuevas specimens were quite volatile to be analyzed in the chamber of the confocal Raman. Thus, no measurements of the powdered samples were carried out with the confocal Raman to prevent the contamination of the analysis chamber and the objective lens.

For each measuring point, the best compromise between the different parameters (acquisition time, number of accumulations and the power of the laser) was optimized to obtain a good spectrum quality. Moreover, the laser power was also controlled to prevent photothermal degradation of the cinnabar ores.

The XRD analyses of the cinnabar minerals and the Pompeian pigment were performed with a PANalytical X'pert PRO powder diffractometer equipped with a copper tube ($\lambda\text{CuK}_{\alpha,\text{mean}} = 1.5418\text{ \AA}$, $\lambda\text{CuK}_{\alpha,1} = 1.54060\text{ \AA}$, $\lambda\text{CuK}_{\alpha,2} = 1.54439\text{ \AA}$), secondary graphite monochromator, automatic sample changer, vertical goniometer (Bragg-Brentano geometry), adjustable divergence aperture and PixCel detector. The angular range (2θ) was scanned between 5° and 70° , while the operating parameters for the Cu tube were 40 kV and 40 mA. The diffractogram data were processed using the X'pert HighScore Plus program. For the analyses, each of the previously mentioned samples was manually pulverized in an agate mortar.

In order to gain knowledge about the morphology of the cinnabar crystals in the mineral ores and in the pigment from Pompeii, an EVO40 Scanning Electron Microscope (SEM) (Carl Zeiss NTS GmbH, Oberkochen, Germany) was used. Moreover, elemental analysis of the samples was also conducted using a X-Max energy dispersive X-ray spectrometer (Oxford Instruments, Abingdon, Oxfordshire, UK) coupled to the SEM. A working distance

of 8.5 mm, a takeoff angle of 35°, and an acceleration voltage of 30 kV were chosen for the elemental analysis. The signal-to-noise ratio of EDS spectra was increased using an integration duration of 50 s. The INCA program (Oxford Instruments, Abingdon, Oxfordshire, UK), able to provide a semi-quantitative assessment of the elements contained in the sample under study, was used for the spectrum data treatment.

3. Results and Discussion

3.1. Mineralogical Characterization of the Cinnabar Ores from the Almadén Mining District

For the identification of the main mineralogical phases of the cinnabar ores from the Almadén mining district, Raman spectroscopy was used. The main Raman bands detected measuring the mineral samples, directly or as isolated powders using the portable instrument, are presented in Table 1, whereas the signals detected with the confocal equipment are summarized in Table 2. A selection of the corresponding Raman spectra is shown in Figure 2 as an example.

Table 1. Raman bands detected on each mineral ore (Almadén, El Entredicho, Las Cuevas) using the portable spectrometer.

Type of Sample	Almadén	El Entredicho	Las Cuevas
Ore fragment	69 (w), 105 (m), 143 (s), 197 (w), 254 (vs), 287 (m), 344 (s), 397 (m), 516 (m), 638 (m), 702 (vw), 1602 (vw), 2069 (vw)	63 (w), 86 (w), 105 (w), 127 (w), 144 (w), 175 (m), 255 (vs), 288 (m), 344 (s), 379 (w), 436 (w), 465 (m), 724 (w), 1096 (s), 1318 (m), 1601 (m)	87 (w), 105 (m), 144 (s), 195 (w), 254 (vs), 287 (m), 344 (s), 394 (m), 513 (m), 638 (m), 709 (vw), 1107 (vw), 1311 (m), 1423 (m), 1601 (m)
Scraped powder	85 (m), 105 (m), 144 (w), 253 (vs), 286 (m), 343 (s)	85 (m), 104 (m), 144 (w), 253 (vs), 286 (m), 343 (s)	84 (m), 104 (m), 144 (w), 253 (vs), 286 (m), 343 (s), 580 (w), 1027 (w), 1187 (w)

vw: very weak, w: weak, m: medium, s: strong, vs: very strong.

Table 2. Raman bands detected on each mineral ore (Almadén, El Entredicho, Las Cuevas) using the confocal Raman spectrometer.

Type of Sample	Almadén	El Entredicho	Las Cuevas
Ore fragment	103 (m), 129 (w), 144 (s), 197 (w), 255 (vs), 287 (m), 344 (s), 397 (m), 465 (m), 516 (m), 639 (m), 1085 (w)	104 (m), 129 (w), 144 (w), 255 (vs), 284 (m), 344 (s), 379 (m), 431 (m), 465 (m)	104 (m), 129 (w), 144 (s), 170 (w), 196 (w), 255 (vs), 287 (m), 344 (s), 465 (m), 578 (w), 637 (m), 707 (w), 1175 (w)

w: weak, m: medium, s: strong, vs: very strong.

According to the work of Nusimovici and Meskaoui, it is possible to attribute many of the bands detected (Table 1) to the different vibration modes of Hg-S. Indeed, the authors observed experimental bands at the following wavenumbers: 65, 87, 106, 178, 255, 283–289, 343, 644, and 707 cm^{-1} [24].

The Raman band at 1100 cm^{-1} , registered in the direct surface measurements from Las Cuevas and El Entredicho specimens, might be related to Si-O-Si asymmetric stretching vibration [25]. Moreover, in these two minerals, the presence of bands around 1300 cm^{-1} and 1600 cm^{-1} could correspond to carbon. In the case of Almadén, only the 1600 cm^{-1} band was noticeable, and it was impossible to confirm the presence of carbon in it.

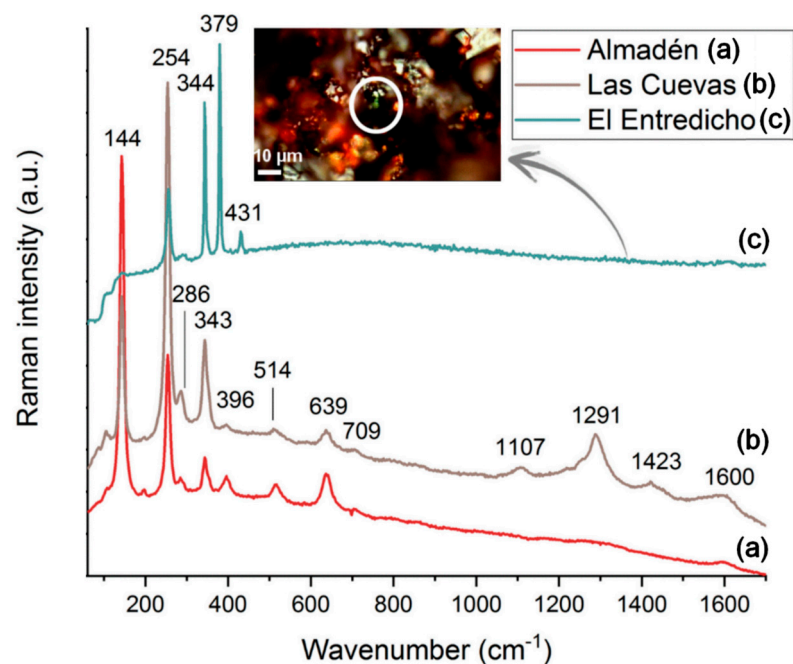


Figure 2. Raman spectra acquired on the surface of the ores of the Almadén mining district using the portable spectrometer (Almadén (a), Las Cuevas (b)) and the confocal instrument (El Entredicho (c)).

The band at around 145 cm^{-1} could be attributed either to cinnabar or to the presence of anatase (TiO_2). The Raman spectrum of anatase is known for its vibrational bands at 144, 197, 399, 513, 639 and 792 cm^{-1} [26,27]. On the mineral fragments of Almadén and Las Cuevas, its bands at around 197, 399, 513, and 639 cm^{-1} are also observable. In El Entredicho, no additional bands of this TiO_2 polymorph were registered, which may suggest that the band at 145 cm^{-1} is related to cinnabar rather than to anatase in this ore. It is notable that the 145 cm^{-1} band is also present in all the scraped powdered samples, a purified form of the cinnabar ore, which reinforces the hypothesis of the attribution of this band to cinnabar and not to anatase in El Entredicho. On the other hand, the $127\text{--}129\text{ cm}^{-1}$ and 465 cm^{-1} bands observed in the spectra acquired in all ores using the confocal instrument can be easily ascribed to α -quartz [28].

In addition, the series of bands at 344, 379, and 431 cm^{-1} , detected in El Entredicho using the confocal instrument, coincide with anisotropic pyrite, distinguishable from isotropic pyrite, which is characterized by Raman bands at 353, 387, and 446 cm^{-1} [29]. The presence of pyrite, common in the Almadén mining district, could have an influence on Pb and S isotopic studies [30,31].

In agreement with the Raman measurements, X-ray diffraction analyses confirmed the occurrence of anatase in Almadén and Las Cuevas, as well as the detection of quartz in all ores, being predominant in El Entredicho (see Figure 3). In this last case, the strong contribution of the $26.63\ 2\theta$ quartz diffraction peak induces a shift in the $26.29\ 2\theta$ cinnabar peak. These observations allow hypothesizing that Almadén and Las Cuevas have a closer mineralogical composition compared with El Entredicho. Other mineral phases observed by XRD were pyrophyllite ($\text{Al}_2\text{Si}_4\text{O}_{10}(\text{OH})_2$) (shown in Figure 3) and kaolinite ($\text{Al}_2\text{Si}_2\text{O}_5(\text{OH})_4$), both in Almadén and Las Cuevas, gypsum ($\text{CaSO}_4 \cdot 2\text{H}_2\text{O}$) in Almadén (shown in Figure 3), and dolomite ($\text{CaMg}(\text{CO}_3)_2$) in El Entredicho.

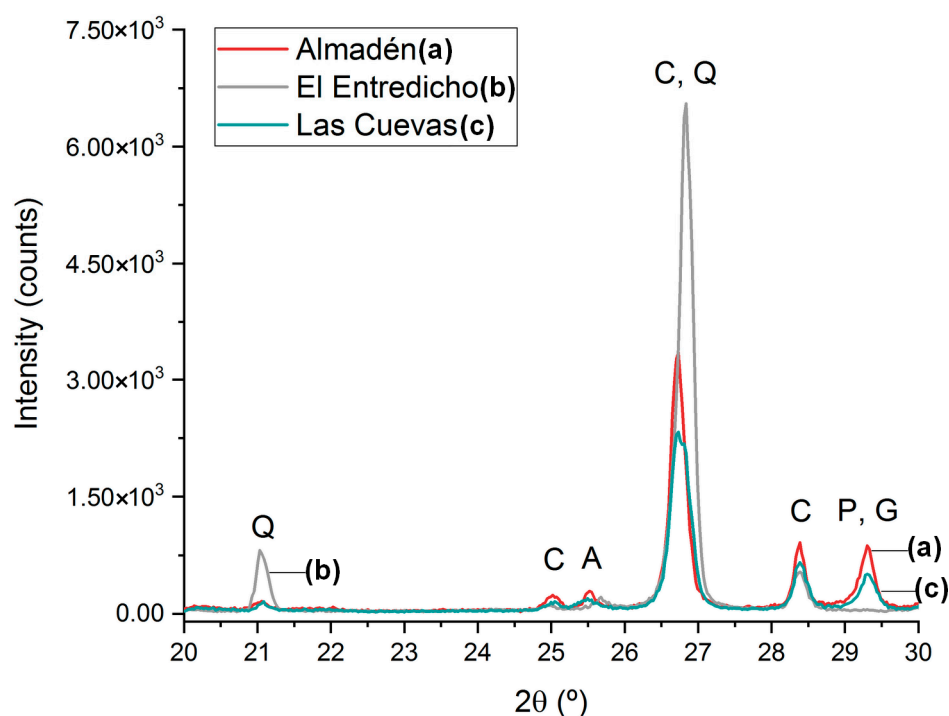


Figure 3. Diffractograms acquired on the samples of the Almadén mining district: Almadén (a), Las Cuevas (b) and (El Entredicho (c). Q: quartz, C: cinnabar, A: anatase, P: pyrophyllite, G: gypsum.

Afterward, a Canonical Discriminant Analysis (CDA) was performed using the Raman spectra acquired on the direct measurements of the mineral samples using the portable instrument (see Figure 4). The values contained in the first ellipse (the smaller one) are in the 95% confidence level, while the other ellipse groups 50% of the observations. This statistical treatment allowed visualizing the differences between known groups. In this case, it confirms that Almadén and El Entredicho have a completely differentiated mineralogical composition, whereas Almadén and Las Cuevas seem to be more correlated. However, among all the measurements acquired on Las Cuevas sample, one of them falls in the 95% confidence ellipse of El Entredicho.

When the cinnabar powders from the veins of the mineral were analyzed, no additional mineral impurities were detected in Almadén and El Entredicho samples (see Table 1). Only the powdered sample from Las Cuevas showed additional unassigned bands at 483, 505, 534, 580, and 1026 cm^{-1} in random spectra.

Finally, using confocal Raman (Table 2), apart from the detection of pyrite, five bands that did not appear in the measurements obtained with the portable instrument were registered: 109, 170, 576, 1056, and 1175 cm^{-1} . Bands at 109 and 170 cm^{-1} can be assigned to cinnabar [24]. The rest of the unassigned bands were detected only in one spectrum. Hence, they cannot be considered representative of the sample. If they are not taken into account, no differences in the results obtained by both instrumentation (portable and confocal) can be appreciated, bearing in mind that pyrite was present as a microcrystal (Figure 2). Consequently, the portable Raman instrument has proven to be as valid as the confocal microscope for the in-situ analysis of cinnabar minerals.

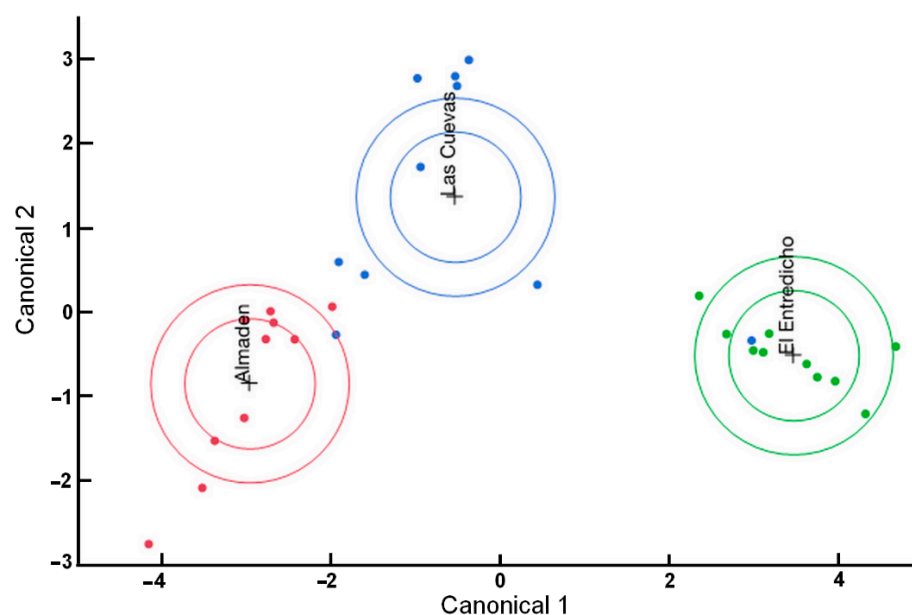


Figure 4. Canonical Discriminant Analysis performed using the spectra acquired directly on the mineral ore fragments with the portable Raman spectrometer.

3.2. Mineralogical Characterization of the Raw Cinnabar Pigment of the Archaeological Park of Pompeii

The raw cinnabar pigment recovered from the excavations of the Archaeological Park of Pompeii was also analyzed by Raman spectroscopy and XRD, in order to evaluate if there existed any mineralogical similarity comparing with the mineral ores of the Almadén mining district. First of all, the morphological appearance of the crystals and their particle size were determined in the scraped powders of the minerals and the historical pigment sample. For that, backscattered electron detection in the SEM was used (Figure 5). As can be appreciated, the historical cinnabar pigment (Figure 5a) seems to be purer and finer than the cinnabar mineral (Figure 5b–d). Figure 6 presents the S (representative of HgS) and Si (indicative of quartz and other silicates, such as pyrophyllite and kaolinite, detected by XRD) EDS maps acquired on the scraped powder from Las Cuevas, which confirm the distribution of the impurities. Apart from that, the Pompeian cinnabar pigment grain size does not exceed 50 μm (see Figure 5a), while the particles in the mineral samples are notoriously bigger.

As Vitruvius and Pliny registered, although the mineral was extracted in Hispania, it was brought to Rome to prepare the precious pigment in manufactories located, according to Vitruvius, between the Temples of Flora and Quirinus. For this aim, the mineral was crushed in iron mortars until a fine powder was obtained, which was successively washed and heated multiple times to ensure the elimination of impurities in the mineral [12]. Accordingly, the BSE micrograph of the Roman pigment proved that the mineral went through a thorough and meticulous purification, as described by Vitruvius.

In good agreement with the SEM observations, the XRD measurements of the archaeological pigment only resulted in the detection of cinnabar, confirming the high purification process conducted to obtain the pigment in Roman times.

Nonetheless, this does not preclude the occurrence of further mineral phases, which could be present below the Limit of Detection (LOD) of this technique (5%).

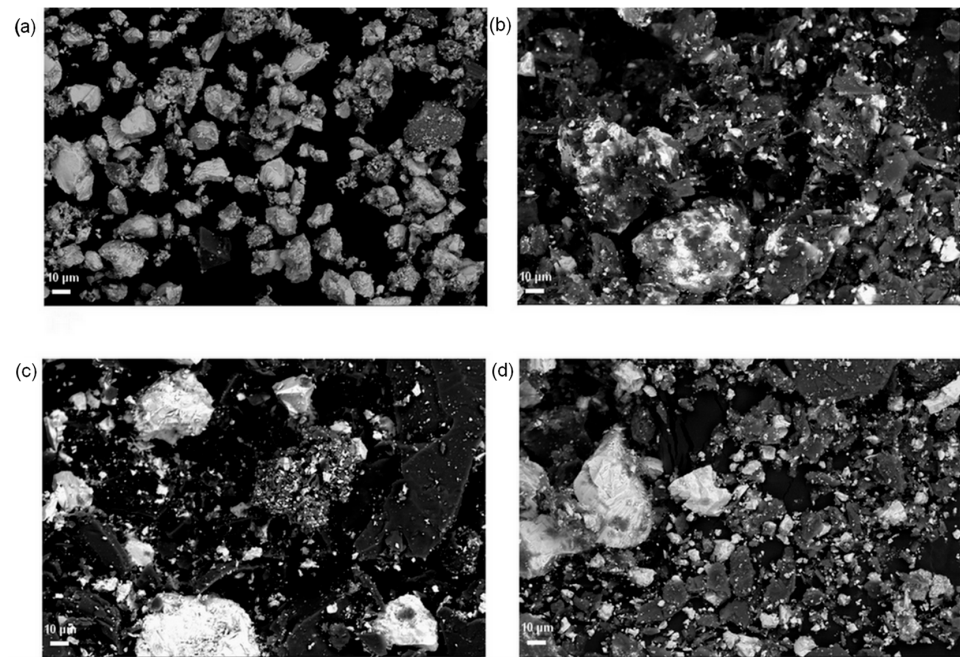


Figure 5. SEM back-scattered electron micrographs of: (a) historical cinnabar pigment of the Archaeological Park of Pompeii, and powder mineral samples of (b) Almadén, (c) Entredicho, and (d) Las Cuevas obtained at the same magnification.



Figure 6. S and Si EDS maps acquired on the powdered mineral sample of Las Cuevas.

The Raman analysis of the pigment allowed the identification of cinnabar, based on the bands at 105, 145, 254, 284, and 344 cm^{-1} . Contrarily to the XRD results, other impurities were also detected (see Figure 7), such as anatase (145, 198, 395, 514 and 638 cm^{-1}), carbon (1300–1600 cm^{-1}), diopside (667 cm^{-1}), gypsum (416, 495, 621, 671, 1008, 1133 cm^{-1}), and calcite (1087 cm^{-1}). Interestingly, Egyptian Blue was found as a contamination of the pigment (see the blue particle in Figure 7) based on the Raman bands at 116, 139, 168, 232, 379, 432, 479, 573, 766, 789, 966, 989, 1014, 1086 and 1145 cm^{-1} [32].

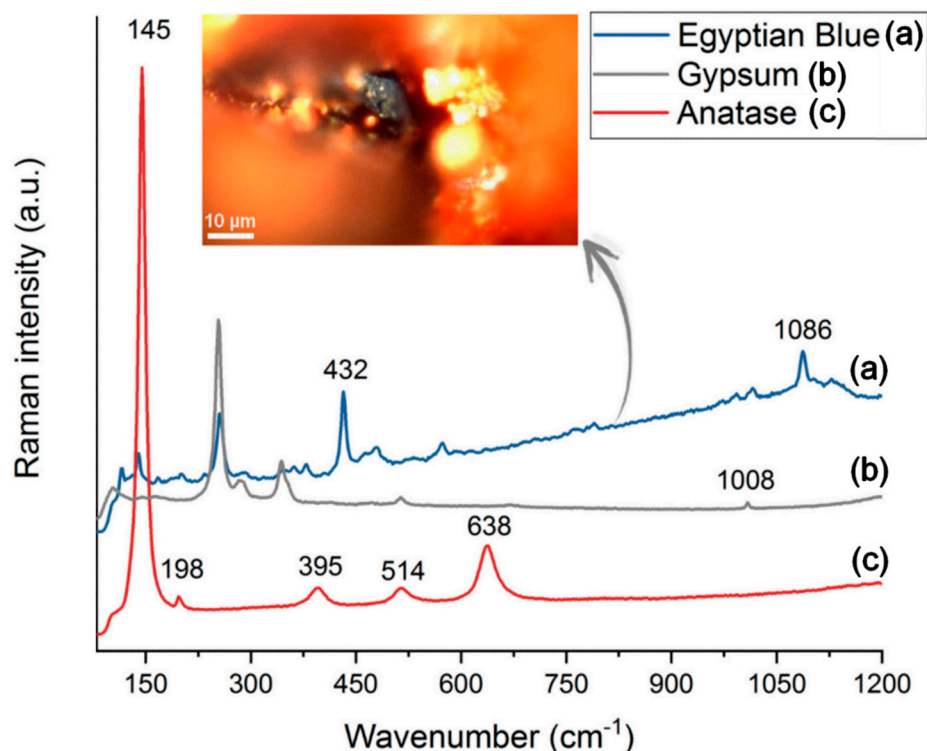


Figure 7. Raman spectra of the impurities found in the raw cinnabar pigment excavated in Pompeii (Egyptian Blue (a), gypsum (b), anatase (c)) and micrograph of the Egyptian Blue grain.

Even though anatase and gypsum were detected by Raman spectroscopy and XRD in the mineral sampled in Almadén as well, this should not be straightforwardly used as a marker of the origin of the pigment. To begin with, anatase has also been found as an impurity, probably of volcanic origin, in yellow ochre pigments excavated in Pompeii [33]. Hence, the presence of anatase in the cinnabar pigment sample could be due to cross-contamination with other locally prepared pigments or volcanic materials of the area, which is in agreement with the detection of diopside. In addition, gypsum is one of the most abundant minerals in S-bearing low-temperature fumaroles of the Somma-Vesuvius volcano [34]. Considering that the cinnabar pigment was impacted by the pyroclastic materials ejected in the 79 AD volcanic eruption, the possible contamination by the pyroclasts cannot be ruled out.

3.3. Identification of Compositional Similarities and Differences among the Cinnabar Mineral Samples and the Pompeian Cinnabar Pigment through EDXRF Spectroscopy

Portable and benchtop EDXRF analyses were performed on the surface of the ore fragments, as well as on the powders extracted from the cinnabar veins, and on the Pompeian cinnabar pigment.

The three mineral fragments contain, apart from Hg and S related to cinnabar, Al, Si, K, Ca, Ti, Fe, Ni, and Zr.

μ -EDXRF elemental maps also helped to evaluate the distribution of the elements on the ores (see Figure 8). Ti and Si accumulations were observed on a fragment from

Almadén (anatase, quartz), as well as the presence of Fe and Si, which could be related to pyrite and quartz, respectively, on a fragment from El Entredicho.

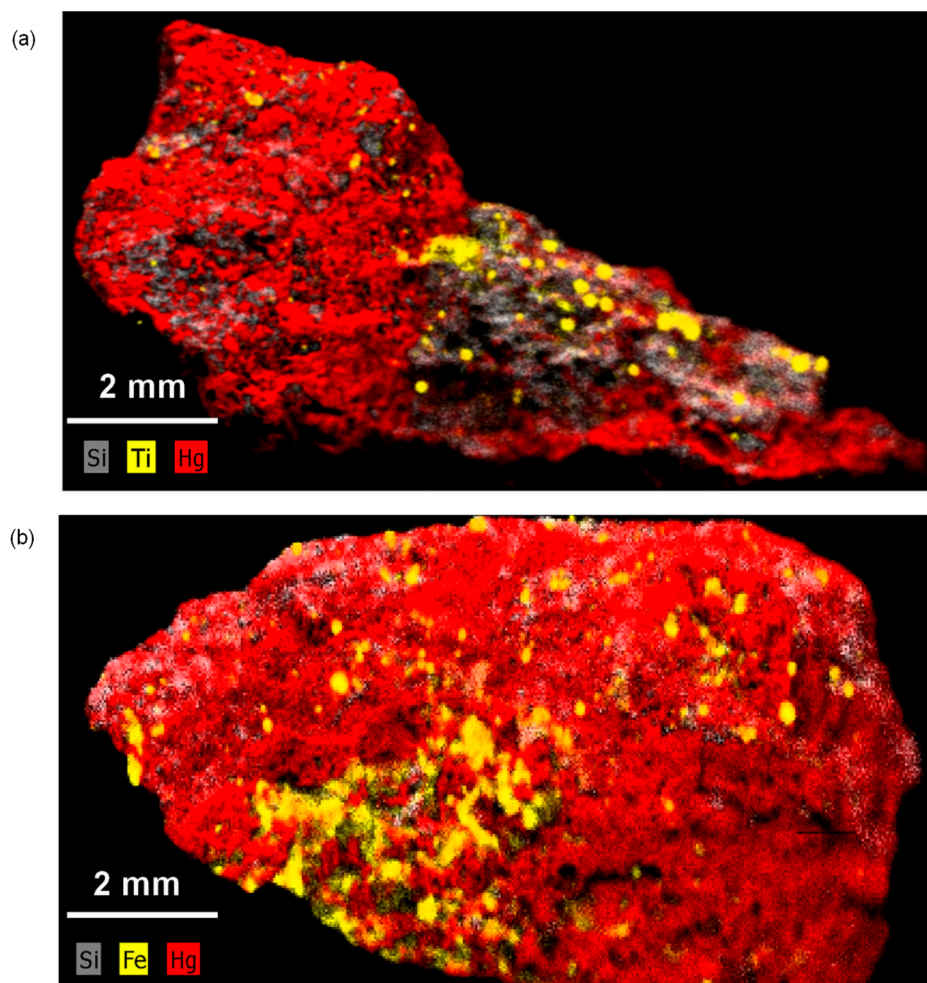


Figure 8. Elemental distribution maps obtained by μ -EDXRF showing (a) the distribution of Hg, Si and Ti on a fragment from the Almadén ore, (b) the distribution of Hg, Si and Fe on a fragment from the El Entredicho ore.

Concerning the Pompeian pigment, the main element that distinguishes this archaeological sample from the three mineral specimens from Almadén is Cu (1100 ± 100 mg/kg), not detected in the mineral ores by EDXRF. As stated in the literature, Cu is present only at trace levels and distributed heterogeneously in the mining district of Almadén in form of chalcopyrite (CuFeS_2) [35]. On the contrary, Cu was identified as almost minor element in the archaeological pigment. Apart from that, the concentrations of Ca and Si are also higher. The increase in the concentration of these three elements is in good agreement with the presence of Egyptian Blue (cuprorivaite, $\text{CaCuSi}_4\text{O}_{10}$), detected by Raman (see Figure 7).

As Cu is associated to Egyptian Blue, this element was removed from the dataset of the semi-quantitative information obtained by the benchtop EDXRF instrument before PCA. In Figure 9a, the scores and loadings plot obtained is presented. As can be appreciated, El Entredicho differs from Las Cuevas and Almadén according to its elemental composition. As clear differences were noticed in the Hg concentrations, an additional PCA with the data of the cinnabar ores was obtained excluding Hg. As can be observed in Figure 9b, a clearer separation of Almadén and Las Cuevas samples from El Entredicho sample was obtained.

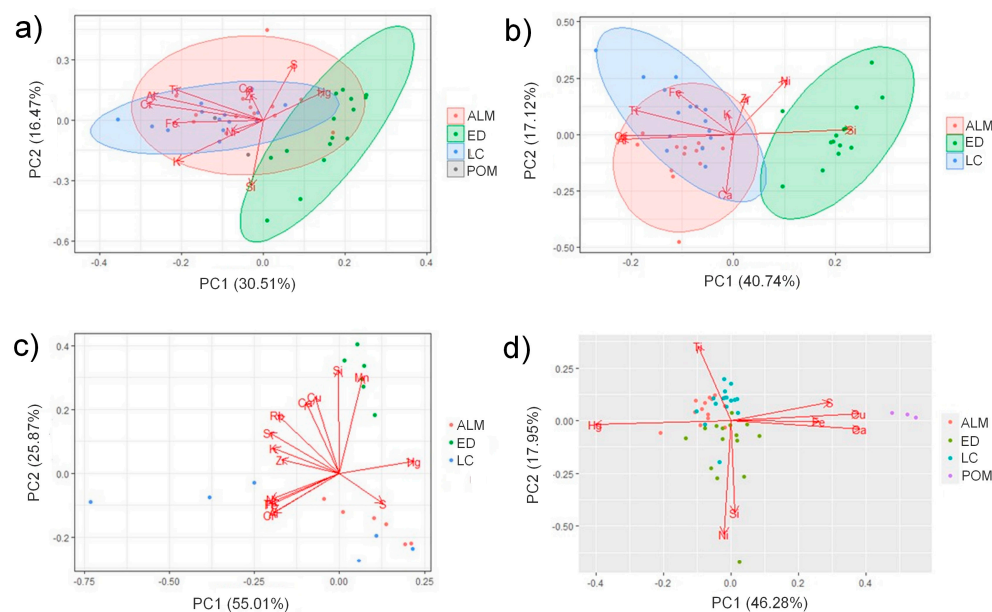


Figure 9. Scores and loadings plot of: (a) the cinnabar ores and the raw pigment from Pompeii using the semi-quantitative dataset from benchtop EDXRF spectrometer, (b) the cinnabar ores using the semi-quantitative dataset from benchtop EDXRF spectrometer excluding Hg, (c) the cinnabar ores using the dataset (normalized counts) from HH-EDXRF spectrometer, (d) the powdered cinnabar ore samples and the raw pigment from Pompeii using the dataset (normalized counts) from benchtop EDXRF spectrometer.

The differences in the elemental composition of Almadén and Las Cuevas samples against El Entredicho are based on the detection of Cr, V, and Ti.

In Figure 9c, the scores and loadings plot obtained for the dataset including the measurements conducted on the ores with the HH-EDXRF spectrometer is presented. As can be observed, the conclusions that might be extracted using the data coming from the portable device are the same comparing with the benchtop instrument. In this case, it was not necessary to consider the exclusion of Hg, maybe due to higher representativeness of the measured points at 8 mm of lateral resolution.

As with the benchtop measurements, in this case, the analyses performed with the HH-EDXRF also revealed that Cr is the main element that differentiates El Entredicho from Almadén and Las Cuevas. Even if Ti was identified in the three ores, its proportion is much higher in Almadén ($166,000 \pm 70,000$ normalized counts) and Las Cuevas ($185,000 \pm 17,000$ normalized counts) than in El Entredicho (8900 ± 4000 normalized counts). Therefore, the higher contribution of Ti also can be considered crucial to distinguish the cinnabar order of El Entredicho from Almadén and Las Cuevas.

Once the elemental differences among the cinnabar minerals coming from different locations inside Almadén mining park were unveiled, an additional PCA was performed using the semi-quantitative results obtained using the benchtop EDXRF spectrometer for the powders isolated from the mineral samples and the historical pigment. As can be observed in Figure 9d, it was possible to separate the four different samples. This result again points to Cr and Ti as key elements to reveal elemental differences between the three mining ores. Therefore, the discrimination of the three mineral samples was based on the presence of Ti in Almadén and Las Cuevas and the absence of this metal in El Entredicho specimen. Finally, the discrimination between Almadén and Las Cuevas is due to the absence of Cr in Almadén compared to Las Cuevas.

4. Conclusions

In this study, relevant results regarding the mineralogical composition of cinnabar ores from the mining district of Almadén and an archaeological pigment found at the Archaeological Park of Pompeii were obtained thanks to XRD analyses, SEM micrographs, and Raman spectroscopy.

Portable and benchtop Raman and EDXRF measurements acquired on the mineral samples can be considered fairly similar in terms of the variety of species/elements detected. This insight supports the reliability of portable instrumentation to perform an in-situ campaign to conduct a general screening of the mineralogy of the Almadén mining park, to select the best candidates for deeper laboratory and isotopic studies. This previous screening step turns out to be crucial to improve the representativeness of the isotopic results, since the values cited in the literature vary greatly depending on the mineral sample extracted from the same mining district.

Thanks to the non-invasive, multianalytical strategy applied in this work, it was possible to differentiate between the minerals sampled in Almadén and Las Cuevas, and those from the El Entredicho. The discrimination is based on the detection of anatase by Raman spectroscopy and XRD in Almadén and Las Cuevas, consistent with the higher intensities of Cr and Ti registered in the EDXRF spectra of these samples. On the contrary, El Entredicho is characterized by the presence of pyrite.

The detection of Egyptian Blue by Raman and Cu, Si, and Ca as minor elements by EDXRF in the original archaeological pigment from Pompeii may arise from contamination during its preparation process (same grinding bowl as Egyptian Blue), the painting procedure, or a later contribution of the burial.

In conclusion, Raman and EDXRF analyses permitted to discern similarities between Almadén and Las Cuevas samples, in contrast to El Entredicho. Unfortunately, no clear correspondence was found between the Pompeian archaeological pigment and the Almadén mineral deposits. However, this observation does not exclude this geological source, since future isotopic studies (Hg or S) are needed to perform a proper provenance study in order to find an unequivocal correlation between the cinnabar mineral of Almadén and the archaeological pigment from Pompeii.

Author Contributions: Conceptualization, C.B., S.P.-D. and M.M.; methodology, C.B., S.P.-D., J.G.I. and M.M.; software, C.B. and M.M.; validation, C.B., S.P.-D. and M.M.; formal analysis, C.B., S.P.-D. and M.M.; investigation, C.B., S.P.-D. and M.M.; resources, C.B., S.P.-D., J.G.I. and M.M.; writing—original draft preparation, C.B. and S.P.-D.; writing—review and editing, C.B., S.P.-D., J.G.I. and M.M.; visualization, C.B. and S.P.-D.; supervision, M.M.; project administration, M.M.; funding acquisition, M.M. All authors have read and agreed to the published version of the manuscript.

Funding: The research leading to these results has received funding from “la Caixa” Foundation (Silvia Pérez-Diez, ID 100010434, Fellowship code LCF/BQ/ES18/11670017). This work has been supported by the project DEMESOS (PES21/85) funded by the University of the Basque Country (UPV/EHU) and project CERIBAM (Grant PID2020-113198GB-I00 funded by MCIN/AEI/10.13039/501100011033 and by “ERDF A way of making Europe”, by the “European Union”).

Data Availability Statement: The data presented in this study are available on request from the corresponding author.

Acknowledgments: The authors are grateful for the technical and human support provided by SGIker (UPV/EHU/ERDF, EU), more concretely to Francisco Javier Sangüesa (General X-ray Service of the UPV/EHU: Rocks and Minerals), Aitor Larrañaga (General X-ray Service of the UPV/EHU: Molecules and Materials), and Alfredo Sarmiento (Coupled Multispectroscopy Singular Laboratory: Raman-LASPEA). Francisco Javier Carrasco-Milara and Ana Conde from Minas de Almadén y Arrayanes S.A (MAYASA) are also thanked for providing the cinnabar minerals and for their collaboration.

Conflicts of Interest: The authors declare no conflict of interest. The funders had no role in the design of the study; in the collection, analyses, or interpretation of data; in the writing of the manuscript, or in the decision to publish the results.

References

1. Martín-Gil, J.; Martín-Gil, F.J.; Delibes-de-Castro, G.; Zapatero-Magdaleno, P.; Sarabia-Herrero, F.J. The First Known Use of Vermillion. *Experientia* **1995**, *51*, 759–761. [CrossRef] [PubMed]
2. Cinnabar, the Ancient Pigment of Mercury. Available online: <https://www.thoughtco.com/cinnabar-the-ancient-pigment-of-mercury-170556> (accessed on 19 December 2019).
3. Tsantini, E.; Minami, T.; Takahashi, K.; Ontiveros, M.Á.C. Analysis of Sulphur Isotopes to Identify the Origin of Cinnabar in the Roman Wall Paintings from Badalona (Spain). *J. Archaeol. Sci. Rep.* **2018**, *18*, 300–307. [CrossRef]
4. Gettens, R.J.; Feller, R.L.; Chase, W.T. Vermilion and Cinnabar. *Stud. Conserv.* **1972**, *17*, 45–69. [CrossRef]
5. Le Fur, D. Les Pigments Dans La Peinture Égyptienne. In *Pigments et Colorants de l'Antiquité et du Moyen Âge: Teinture, peinture, enluminure, études historiques et physico-chimiques*; CNRS Éditions: Paris, France, 1990; pp. 181–188.
6. Harris, C.D. *Cinnabar: The Symbolic, Seductive, Sublethal Shade of Pompeii*; Brandeis University: Waltham, MA, USA, 2015.
7. Trinquier, J. Cinnabaris et « Sang-Dragon »: Le « Cinabre » Des Anciens Entre Minéral, Végétal et Animal. *Rev. Archéol.* **2013**, *56*, 305–346. [CrossRef]
8. Sharples, R.W. *Theophrastus of Eresus: Life, Writings, Various Reports, Logic, Physics, Metaphysics, Theology, Mathematics*; Brill: Leiden, The Netherlands, 1998.
9. *The Natural History of Pliny*; Henry George Bohn: London, UK, 1855.
10. Nöller, R. Cinnabar Reviewed: Characterization of the Red Pigment and Its Reactions. *Stud. Conserv.* **2015**, *60*, 79–87. [CrossRef]
11. Spangenberg, J.E.; Lavrič, J.V.; Meisser, N.; Serneels, V. Sulfur Isotope Analysis of Cinnabar from Roman Wall Paintings by Elemental Analysis/Isotope Ratio Mass Spectrometry—Tracking the Origin of Archaeological Red Pigments and Their Authenticity. *Rapid Commun. Mass. Spectrom.* **2010**, *24*, 2812–2816. [CrossRef]
12. Vitruvius. The Architecture of Marcus Vitruvius Pollio. In *Ten Books*; Priestley and Weale: London, UK, 1826.
13. Hernández, A.; Jébrak, M.; Higuera, P.; Oyarzun, R.; Morata, D.; Munhá, J. The Almadén Mercury Mining District, Spain. *Miner. Deposita* **1999**, *34*, 539–548. [CrossRef]
14. Gray, J.E.; Pribil, M.J.; Higuera, P.L. Mercury Isotope Fractionation during Ore Retorting in the Almadén Mining District, Spain. *Chem. Geol.* **2013**, *357*, 150–157. [CrossRef]
15. Eastaugh, N.; Walsh, V.; Chaplin, T.; Siddall, R. *Pigment Compendium—A Dictionary and Optical Microscopy of Historical Pigments*; Routledge: Oxford, UK, 2008.
16. Miguel, C.; Pinto, J.V.; Clarke, M.; Melo, M.J. The Alchemy of Red Mercury Sulphide: The Production of Vermilion for Medieval Art. *Dyes. Pigm.* **2014**, *102*, 210–217. [CrossRef]
17. Elert, K.; Cardell, C. Weathering Behavior of Cinnabar-Based Tempera Paints upon Natural and Accelerated Aging. *Spectrochim. Acta. A. Mol. Biomol. Spectrosc.* **2019**, *216*, 236–248. [CrossRef]
18. Higuera, P.; Munhá, J.; Oyarzun, R.; Tassinari, C.C.G.; Ruiz, I.R. First Lead Isotopic Data for Cinnabar in the Almadén District (Spain): Implications for the Genesis of the Mercury Deposits. *Miner. Deposita* **2005**, *40*, 115–122. [CrossRef]
19. Mazzocchin, G.A.; Baraldi, P.; Barbante, C. Isotopic Analysis of Lead Present in the Cinnabar of Roman Wall Paintings from the Xth Regio “(Venetia et Histria)” by ICP-MS. *Talanta* **2008**, *74*, 690–693. [CrossRef] [PubMed]
20. Marcaida, I.; Maguregui, M.; Morillas, H.; García-Florentino, C.; Knuutinen, U.; Carrero, J.A.; Fdez-Ortiz de Vallejuelo, S.; Pitarch Martí, A.; Castro, K.; Madariaga, J.M. Multispectroscopic and Isotopic Ratio Analysis To Characterize the Inorganic Binder Used on Pompeian Pink and Purple Lake Pigments. *Anal. Chem.* **2016**, *88*, 6395–6402. [CrossRef]
21. Trentin, S. Reality, Artifice and Changing Landscapes in the House of Marcus Lucretius in Pompeii. *Greece Rome* **2019**, *66*, 71–92. [CrossRef]
22. Seiler, F.; Grunwald, P.; Gut, W.; Diederichs, H.; Sellers, J. *Casa Degli Amorini Dorati (VI 16, 7, 38)*; Häuser in Pompeji: Hirmer, München, 1992; ISBN 978-3-7774-5450-4.
23. Database of Raman Spectroscopy, X-ray Diffraction and Chemistry of Minerals. Available online: <https://rruff.info/> (accessed on 26 December 2022).
24. Nusimovici, M.A.; Meskaoui, A. Raman Scattering by α -HgS (Cinnabar). *Phys. Status Solidi B* **1973**, *58*, 121–125. [CrossRef]
25. Yadav, A.K.; Singh, P. A Review of the Structures of Oxide Glasses by Raman Spectroscopy. *RSC Adv.* **2015**, *5*, 67583–67609. [CrossRef]
26. Ohsaka, T.; Izumi, F.; Fujiki, Y. Raman Spectrum of Anatase, TiO₂. *J. Raman Spectrosc.* **1978**, *7*, 321–324. [CrossRef]
27. Murad, E. Identification of Minor Amounts of Anatase in Kaolins by Raman Spectroscopy. *Am. Mineral.* **1997**, *82*, 203–206. [CrossRef]
28. Krishnan, R.S. Raman Spectrum of Quartz. *Nature* **1945**, *155*, 452. [CrossRef]
29. Mernagh, T.P.; Trudu, A.G. A Laser Raman Microprobe Study of Some Geologically Important Sulphide Minerals. *Chem. Geol.* **1993**, *103*, 113–127. [CrossRef]
30. Jébrak, M.; Higuera, P.L.; Marcoux, É.; Lorenzo, S. Geology and Geochemistry of High-Grade, Volcanic Rock-Hosted, Mercury Mineralisation in the Nuevo Entredicho Deposit, Almadén District, Spain. *Miner. Deposita* **2002**, *37*, 421–432. [CrossRef]
31. Saupé, F.; Arnold, M. Sulphur Isotope Geochemistry of the Ores and Country Rocks at the Almadén Mercury Deposit, Ciudad Real, Spain. *Geochim. Cosmochim. Acta* **1992**, *56*, 3765–3780. [CrossRef]
32. Luque, L.D.M.; Ruiz, J.R. Análisis de pigmentos por espectroscopia Raman de la “villa” romana de El Ruedo (Almedinilla, Córdoba). *Antiquitas* **2015**, *27*, 69–85.

33. Marcaida, I.; Maguregui, M.; Morillas, H.; Veneranda, M.; Prieto-Taboada, N.; Fdez-Ortiz de Vallejuelo, S.; Madariaga, J.M. Raman Microscopy as a Tool to Discriminate Mineral Phases of Volcanic Origin and Contaminations on Red and Yellow Ochre Raw Pigments from Pompeii. *J. Raman Spectrosc.* **2019**, *50*, 143–149. [[CrossRef](#)]
34. Balassone, G.; Petti, C.; Mondillo, N.; Panikorovskii, T.L.; de Gennaro, R.; Cappelletti, P.; Altomare, A.; Corriero, N.; Cangiano, M.; D’Orazio, L. Copper Minerals at Vesuvius Volcano (Southern Italy): A Mineralogical Review. *Minerals* **2019**, *9*, 730. [[CrossRef](#)]
35. Hunt-Ortiz, M.A.; Consuegra-Rodríguez, S.; Díaz del Río-Español, P.; Hurtado-Pérez, V.M.; Montero-Ruiz, I. Neolithic and Chalcolithic –VI to III Millennia BC—Use of Cinnabar (HgS) in the Iberian Peninsula: Analytical Identification and Lead Isotope Data for an Early Mineral Exploitation of the Almadén (Ciudad Real, Spain) Mining District. In *Proceedings of the History of Research in Mineral Resources, Madrid, Spain, 1–14 July 2010*; Instituto Geológico y Minero de España: Madrid, Spain; Volume 13, pp. 3–13.

Disclaimer/Publisher’s Note: The statements, opinions and data contained in all publications are solely those of the individual author(s) and contributor(s) and not of MDPI and/or the editor(s). MDPI and/or the editor(s) disclaim responsibility for any injury to people or property resulting from any ideas, methods, instructions or products referred to in the content.